

See discussions, stats, and author profiles for this publication at: <https://www.researchgate.net/publication/27708327>

Effect of Size and Extent of Sulfation of Bulk and Silica-Supported ZrO₂ on Catalytic Activity in Gas- and Liquid-Phase Reactions

ARTICLE *in* THE JOURNAL OF PHYSICAL CHEMISTRY B · DECEMBER 2003

Impact Factor: 3.3 · DOI: 10.1021/jp030436b · Source: OAI

CITATIONS

10

READS

20

3 AUTHORS, INCLUDING:



J.W. Geus

Utrecht University

392 PUBLICATIONS 8,271 CITATIONS

SEE PROFILE

Effect of Size and Extent of Sulfation of Bulk and Silica-Supported ZrO₂ on Catalytic Activity in Gas- and Liquid-Phase Reactions

Ivo J. Dijs, John W. Geus, and Leonardus W. Jenneskens*

Debye Institute, Department of Physical Organic Chemistry, Utrecht University, Padualaan 8, 3584 CH Utrecht, The Netherlands

Received: April 11, 2003; In Final Form: September 29, 2003

Sulfated zirconia has been prepared according to three different procedures, viz., (i) conventional impregnation with sulfuric acid and calcination (3 h at 773 K) of two zirconia's (50 and 217 m²/g), (ii) reaction of zirconium tetrachloride with sulfuric acid giving bulk anhydrous zirconium sulfate, and (iii) deposition–precipitation of highly dispersed zirconia on silica and subsequent reaction with either H₂S and O₂, or SO₂ and O₂, or SO₃. The latter two procedures lead to essentially water-free catalysts. Thermogravimetry showed that the impregnated and calcined zirconia's loose sulfate above 830 K (50 m²/g) and 910 K (217 m²/g). In a gas flow containing water, the sulfated silica-supported zirconia loses sulfate already at 673 K because of the reaction to more volatile sulfuric acid. The catalysts were employed in the gas-phase trans-alkylation of benzene (**1**) and diethylbenzene (**2**) to ethylbenzene (**3**) at 473 and 673 K and in the solvent-free, liquid-phase hydroacyloxy-addition of acetic acid to camphene (**4**) to camphene (**5**) to isobornyl acetate (**6**) at 338 K. The water-free catalysts were not active; only after addition of water was catalytic activity exhibited. The catalytic activity of the differently prepared sulfated zirconia's is governed by the equilibrium: $\text{Zr}(\text{SO}_4)_2 + 4\text{H}_2\text{O} \rightleftharpoons \text{Zr}(\text{SO}_4)_2 \cdot 4\text{H}_2\text{O} + n\text{H}_2\text{O} \rightleftharpoons \text{ZrO}_2 + 2\text{H}_2\text{SO}_4\cdot\text{aq}$. Addition of water vapor to the bulk sulfate at 473 K led to the reaction to the tetrahydrate, which was not active, whereas the highly dispersed silica-supported zirconium sulfate reacted to form sulfuric acid. The supported catalyst rapidly released the water at 473 K, which resulted in a rapid drop in catalytic activity. Transport of water through the porous system dominates the activity of the impregnated zirconia's. Accordingly, the slight activity of the zirconia of 50 m²/g rapidly dropped at 473 K, whereas the zirconia of 217 m²/g displayed a high and stable activity. At 673 K, the transport is much more rapid. The activity of the highly porous zirconia was therefore at 673 K much lower than at 473 K. Whereas the gas-phase reaction is governed by transport of water vapor, the liquid-phase reaction is dominated by transport of the reactants to the active sites. Consequently, the sulfated zirconia of 50 m²/g showed a considerably higher activity than that of 217 m²/g. Also the silica-supported catalyst exhibited a higher activity. The consistent results demonstrate that sulfated zirconia needs water to display activity in the gas-phase and liquid-phase reaction studied.

Introduction

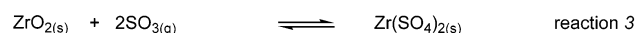
Homogeneous, corrosive liquid acid catalysts, such as BF₃ complexes and H₂SO₄, are still frequently employed in the production of (fine) chemicals.^{1,2} Replacement of the acids by a solid catalyst is desirable to achieve more effective catalyst handling and product purification and to diminish waste production.^{1,3} In the last two decades, “sulfated metal oxides” have received considerable attention as potentially benign solid acid catalysts that possess a very high activity and even superacidity.^{1,3–5} Despite the promising properties, technical applications¹ are still lacking, which is due to the activity being difficult to control in view of, for example, the sensitivity to hydration,^{6,7} the thermal stability,^{8,9} and an interference of reduction processes.^{10–17}

In this research, we focused on sulfated zirconia, in which the following equilibria are dominating: $\text{Zr}(\text{SO}_4)_2 + 4\text{H}_2\text{O} \rightleftharpoons \text{Zr}(\text{SO}_4)_2 \cdot 4\text{H}_2\text{O} + n\text{H}_2\text{O} \rightleftharpoons \text{ZrO}_2 + 2\text{H}_2\text{SO}_4\cdot\text{aq}$. The usual impregnation of zirconia with sulfuric acid, drying, and calcination brings about that the activity of sulfated zirconia is difficult

to control,^{3–5,18,19} a procedure resulting in a material of a heterogeneous and complex structure.^{4–7,20–24} As indicated by the above equilibria, impregnation with a relatively large amount of diluted sulfuric acid and drying leads to dissolved zirconium sulfate, which crystallizes to $\text{Zr}(\text{SO}_4)_2 \cdot 4\text{H}_2\text{O}$ upon further drying. The hydrated sulfate may be locally deposited within the porous zirconia. With pore-volume impregnation reaction to $\text{Zr}(\text{SO}_4)_2 \cdot 4\text{H}_2\text{O}$ is less likely. The water remaining after drying will lead to the presence of bisulfate (–OSO₃H) or sulfuric acid on the zirconia surface.

Starting with zirconium sulfate of a low surface area, the above equilibria will only involve reaction to $\text{Zr}(\text{SO}_4)_2 \cdot 4\text{H}_2\text{O}$ and $\text{Zr}(\text{SO}_4)_2$. The water leading to the reaction to sulfuric acid will be rapidly removed at a low temperature, where loss of sulfate will not significantly proceed. Figure A4 of the Supporting Information, which represents the phase diagram of sulfuric acid, confirms the conclusion. Up to a temperature of about 473 K, the gas phase only involves water. Only at higher temperatures does the gas phase contain increasingly the constituents of sulfuric acid, viz., H₂O, SO₃, SO₂, and O₂. Because water-free bulk zirconium sulfate loses sulfate only at temperatures above 890 K,⁶ a rapid transport of water smoothly

* To whom correspondence should be addressed: Tel: +31-302533128. Fax: +31-302534533. E-mail: jenneskens@chem.uu.nl.

CHART 1: Gas-Phase Sulfation of ZrO₂ by H₂S/O₂, SO₂/O₂, or SO₃

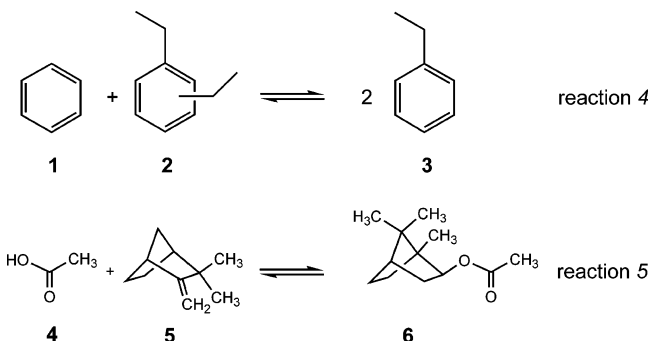
leads to Zr(SO₄)₂. With a highly porous zirconia, on the other hand, which has been impregnated with diluted sulfuric acid, a sufficiently rapid transport of water out of the porous system may call for temperatures thus high, so that the vapor phase also contains significant amounts of the constituents of sulfuric acid.

The possible loss of sulfate brings about that the catalytic activity of sulfated zirconia does not depend on the final temperature during drying and calcination. The heating rate is highly important as well as the total amount of sulfated zirconia thermally treated. Release of water and the constituents of sulfuric acid from a large batch is much more difficult than that from a small sample. Application of a gas flow can also affect the final activity, and with large batches treated in a fixed bed, an inhomogeneous catalyst may result.

First of all, we established the catalytic activity of water-free zirconium sulfate. In view of the low surface-to-volume ratio of bulk zirconium sulfate,⁶ we prepared also water-free, finely divided silica-supported zirconium sulfate. The effect of addition of water vapor on the activity of the water-free catalysts was also investigated. To elucidate the influence of the conditions during drying and calcination, we compared the activity of conventionally prepared sulfated zirconia's with that of the initially water-free catalysts. Because the rate of transport of water out of the porous system may severely affect the loss of sulfate, we prepared two sulfated zirconia's of a considerably different porous structure (50 m²/g and 217 m²/g) according to the conventional procedure, viz., impregnation with diluted sulfuric acid, drying, and calcination.

We recently reported about the preparation of anhydrous Zr(SO₄)₂.⁶ Deposition—precipitation was employed to apply zirconia on a nonporous silica support (50 m²/g).²⁵ Three different procedures (Chart 1) were investigated to react the supported zirconia to water-free zirconium sulfate, viz., treatment with H₂S and subsequent with O₂, reaction with SO₂ and O₂, and reaction with SO₃ produced by in situ oxidation of SO₂ with O₂ on a Pt/SiO₂ catalyst. Thermodynamics (Ellingham diagrams: see the Supporting Information Figure A1) indicates that Δ*G* is slightly positive for the reaction to ZrS₂ (reaction 1a). An excess of H₂S is thus required to get significant sulfidation of ZrO₂. Reaction 1b, oxidation to the corresponding sulfate, is thermodynamically much more favorable. Nevertheless, sulfation by treatment with either SO₂/O₂ or SO₃/SO₂/O₂ (reactions 2 and 3) is preferred, because they can be performed in one step without introducing water.²⁶

The prepared catalysts were thoroughly characterized by XRD, XPS, SEM-EDX, and elemental analysis. Thermogravimetry can provide important information about the reaction to bulk of surface zirconium sulfate. Whereas volatilization of sulfuric acid calls for a temperature above about 500 K, the decomposition of zirconium sulfate has been indicated above to proceed at much more elevated temperatures. When impregnation with sulfuric acid, drying, and calcination does not lead to zirconium sulfate, but due to the presence of water to essentially supported sulfuric acid, release of the constituents of sulfuric acid can be expected above about 500 K. Transport

CHART 2: Gas-Phase Trans-Alkylation of Benzene (1) and Diethylbenzene (2), Giving Two Mol Equivalents of Ethylbenzene (3) (Reaction 4), and the Liquid-Phase Hydro-Acyloxy-Addition Reaction of Acetic Acid (4) to Camphene (5), Giving Isobornyl Acetate (6) (Reaction 5)

through the pores of the zirconia will determine the loss of water and sulfate of the impregnated zirconia.

The properties and catalytic behavior of the three differently prepared catalysts are compared in the gas-phase trans-alkylation reaction of benzene (1) and diethylbenzene (2) giving ethylbenzene (3) as well as in the liquid-phase hydro-acyloxy-addition reaction of acetic acid (4) with camphene (5) giving isobornyl acetate (6) as major product (Chart 2; reactions 4^{27–30} and 5^{2,27,31–34}).

The gas phase reaction has been studied at 473 and 673 K. At 473 K, volatilization of water will dominate, whereas at 673 K, both water and sulfuric acid will desorb. Because the reactants and the reaction products of the gas-phase reaction do not adsorb strongly on the surface of the (sulfated) zirconia, transport limitations are not likely. Transport within the liquid phase proceeds much slower than in the gas phase. The accessibility of the sulfated zirconia species therefore can be expected to dominate the activity in the liquid phase. The sulfated zirconia of 50 m²/g and the silica-supported sulfated zirconia catalyst are therefore likely to exhibit the most elevated activity with a liquid-phase reaction.

Experimental Section

General. ICP-AES (Thermo Jarrell Ash, Atomscan-16 equipped with a photomultiplier detector) was used to analyze the elements Zr and Si. Prior to analysis, the sample was mixed with Li₂B₄O₇ and melted in a carbon cup to give a glass bead, which was subsequently dissolved in concentrated HNO₃. Sulfur (S) was analyzed as SO₂ using a Carlo Erba NA-1500 (Fisons-CE Instruments) NCS-analyzer equipped with a flash-combustion chamber, a Porapak QS 1.83 m × 4 mm column and a TCD. For flash-combustion GC analyses, the samples were mixed with V₂O₅ in a small tin container, sealed, and subsequently combusted in an excess of O₂ (flash-combustion). With a He flow, the evolved SO₃ was passed through a reduced Cu column to reduce SO₃ to SO₂. Before separation on the GC column, the gases were dried over Mg(ClO₄)₂.

Powder XRD patterns were recorded with an Enraf/Nonius FR 590 X-ray powder diffractometer equipped with a Co anode (Kα 1.78897 Å) and an Inel CPS120 (Ar/C₂H₄) curved position-sensitive detector; a reflectometry-sample-holder was used. After subtraction of the scattering background, the volume-averaged diameter of crystallites was calculated from the fwhm using the Scherrer formula (see the Supporting Information; eq A1).³⁵

Specific surface areas of the catalysts were determined by measuring N₂ adsorption–desorption isotherms at 77 K using

a Micrometrics ASAP 2400 apparatus (equilibration interval 15 s) according to the BET approach.³⁶ Prior to the measurements, the samples (ca. 1 g) were evacuated at 393 K for 16 h.

XPS analysis was performed on a Vacuum Generators (Fisons Instruments) MT-500 with a nonmonochromatic Al X-ray source ($K\alpha$ 1486.6 keV) and a CLAM-2 hemispherical analyzer for electron detection. The samples were supported on carbon adhesive tape. Spectra were corrected for charging using the Si(2p) peak and scaled on the Si(2s) peak. For the determination of the binding energies, a background correction was applied.³⁷

The thermal stability of the catalysts was assessed by analyzing the relative loss of weight in a dry N_2 flow (50 mL/min) as a function of temperature and time with a (PC-controlled) Perkin-Elmer TGS-2 TGA apparatus, autobalance AR-2. Temperature program: 1 h at 323 K, heating rate 10 K/min to 1123 K followed by 15 min at 1123 K. Samples of ca. 3.5 mg were used.

TEM analysis was performed with a Philips EM420 electron microscope and a Philips CM200 transmission electron microscope equipped with an EDAX detector for elemental analysis. Copper grids covered by a thin polymer film on which carbon was deposited were used as supports for the ground and ultrasonically dispersed (in dry *n*-hexane) samples.

A Philips XL 30 FEG scanning electron microscope equipped with an EDAX detector for elemental analysis provided SEM images of the catalysts and the local element composition. The samples were supported on carbon adhesive tape and covered with a carbon layer by vapor deposition for electrical conductance.

Catalyst Preparation. Two homogeneous deposition-precipitation methods were evaluated for the preparation of 10 wt % $\text{ZrO}_2/\text{SiO}_2$ catalyst precursors.

Precipitation of ZrO_2 on Silica by Hydrolysis of Urea. A reaction vessel (2 L) equipped with a pH meter, thermometer, baffles, and a mechanical stirrer (1000 rpm) was charged with 13.5 g (0.225 mol) of SiO_2 [Aerosil OX50 (Degussa-Hüls), surface area 50 m^2/g], 4.0 M HCl (500 mL), and 3.92 g (12.2 mmol) of $\text{ZrOCl}_2 \cdot 8\text{H}_2\text{O}$, dissolved in 4.0 M HCl (250 mL). Subsequently, 185 g (3.08 mol) of urea dissolved in 4.0 M HCl (250 mL) was added, and the reaction mixture was heated to 363 K. At this temperature, hydroxyl ions are homogeneously generated by the hydrolysis of urea.^{38,39} After 3 days, a constant pH of 6.0 was reached (measured separately at 293 K) and the suspension was filtered. Because the resulting dispersion of ZrO_2 on the silica support can be affected by calcination (both water and salts may react with the precipitated material to give volatile compounds),⁴⁰ the wet residue was re-suspended three times in water (300 mL) for 1 day followed by filtration in order to remove remaining NH_4Cl impurities. The final residue was dried at 393 K for 1 day and subsequently sieved; the 500–850 μm fraction was isolated. Calcination was performed under carefully controlled conditions using a quartz fixed bed reactor (i.d. 10 mm) equipped with a K-type thermocouple. The 500–850 μm sieve fraction was calcined at 723 K for 10 h (heating/cooling rate: 5 K/min) in a dry air flow (50 mL/min). On top of the sieve fraction, glass beads ($d = 1.0$ mm) were placed to achieve effective preheating of the air flow. The 10 wt % $\text{ZrO}_2/\text{SiO}_2$ catalyst precursor was isolated from the calcination reactor and stored under dry air.

pH-Static Precipitation of ZrO_2 on Silica. In a reaction vessel (2 L) equipped with a pH-meter, thermometer, baffles, and a stirrer (1000 rpm), 13.5 g (0.225 mol) of SiO_2 [Aerosil OX50 (Degussa-Hüls), 50 m^2/g] was suspended in 750 mL of water. Under stirring, both 4.0 M HCl and 4.0 M NH_3 were separately

injected via narrow tubes (i.d. = 1.0 mm) ending below the level of the liquid using two Gilson Minipuls III peristaltic pumps. Whereas the 4.0 M HCl was injected at a rate of 0.25 mL/min, the injection of the 4.0 M NH_3 solution was automatically regulated to maintain a pH of 4.5. When a constant pH of 4.5 was reached, the 4.0 M HCl was replaced by a 4.0 M HCl (250 mL) solution containing 3.92 g (12.2 mmol) of $\text{ZrOCl}_2 \cdot 8\text{H}_2\text{O}$. After addition of these solutions, the pH was raised to 6.5 with the 4.0 M NH_3 solution. The workup and calcination procedures for the 10 wt % $\text{ZrO}_2/\text{SiO}_2$ dispersion were the same as those for the preparation employing the hydrolysis of urea described above. The 10 wt % $\text{ZrO}_2/\text{SiO}_2$ catalyst precursor was removed from the calcination reactor and stored under dry air.

Gas-Phase Sulfation of 10 wt % $\text{ZrO}_2/\text{SiO}_2$ Catalyst Precursors. Three different gas-phase sulfation procedures were used: treatments of 10 wt % $\text{ZrO}_2/\text{SiO}_2$ with (i) H_2S followed by oxidation with O_2 (acronym: $\text{H}_2\text{S}/\text{O}_2$), (ii) SO_2 and O_2 (acronym: SO_2/O_2), and (iii) SO_2 and O_2 , but with a Pt/ SiO_2 catalyst to generate SO_3 in situ (acronym: $\text{SO}_3/\text{SO}_2/\text{O}_2$). Gas purities were He 99.995%, H_2S 99.6%, SO_2 99.9%, O_2 99.999%, and N_2 99.999%. The gas-phase sulfation reactions were performed in a quartz fixed-bed reactor (i.d. 10 mm) equipped with a K-type thermocouple. Helium (He) was used to maintain a gas flow of 50 mL/min. Glass beads ($d = 1.0$ mm) were placed on top of the silica-supported metal oxide particles (500–850 μm sieve fraction) to achieve effective preheating of the gas flow. Via a heat-traced tube (423 K), the gas-flow leaving the reactor was passed through a stirred suspension of $\text{Ca}(\text{OH})_2$ in water. For a schematic representation of the reactor see the Supporting Information (Figure A2). The treated 10 wt % $\text{ZrO}_2/\text{SiO}_2$ catalysts were removed from the reactor and stored under dry air prior to analysis and application.

(1) $\text{H}_2\text{S}/\text{O}_2$: 0.7 g of the 500–850 μm sieve fraction of the 10 wt % $\text{ZrO}_2/\text{SiO}_2$ precursors was heated under He to 623 K at 5 K/min. Subsequently, H_2S (2.5 vol %) was passed through the reactor for 2 h, after which the reactor was purged with He for 30 min. Next, O_2 (20 vol %) was passed through for 2 h, after which the catalyst was cooled to room temperature at 5 K/min under a He flow (50 mL/min).

(2) SO_2/O_2 : 0.7 g of the 10 wt % $\text{ZrO}_2/\text{SiO}_2$ precursors (500–850 μm sieve fraction) was heated under He to 673 K at 5 K/min. Next, SO_2 (5 vol %) and O_2 (5 vol %) were passed through the reactor for 5.5 h after which the temperature was lowered to 573 K. Subsequently, the temperature was lowered to room temperature at 5 K/min under a He flow (50 mL/min).

(3) $\text{SO}_3/\text{SO}_2/\text{O}_2$: With the exception of the addition of a layer of a finely powdered 2 wt % Pt/ SiO_2 oxidation catalyst at half-height of the glass bead layer, the SO_2/O_2 procedure was applied. The oxidation catalyst converts part of the SO_2 into SO_3 (50% based on BaSO_4 precipitation and UV–Vis analysis) before reaching the 10 wt % $\text{ZrO}_2/\text{SiO}_2$.

Calcined H_2SO_4 –Impregnated ZrO_2 Catalysts. Calcined H_2SO_4 –impregnated ZrO_2 catalysts (acronym: $\text{H}_2\text{SO}_4/\text{ZrO}_2$) were prepared following a literature procedure;¹⁹ two different ZrO_2 sources were used.

(1) Precipitated ZrO_2 [acronym: $\text{ZrO}_2(\text{prec.})$] 20.23 g (62.8 mmol) of $\text{ZrOCl}_2 \cdot 8\text{H}_2\text{O}$ was dissolved in water (160 mL), and under vigorous stirring, 25 wt % NH_3 was added dropwise until pH = 8. Next, NH_4Cl was removed by four times re-suspending the wet residue in water (300 mL) for 1 day followed by filtration. The $\text{ZrO}_2(\text{prec.})$ was dried at 433 K for 16 h.

(2) Commercial ZrO_2 : Gimex B. V. [acronym: ZrO_2 –(Gimex)], The Netherlands, surface area 60 m^2/g , monoclinic.

Sulfation of both zirconia's was performed by stirring 4.0 g (32.46 mmol) of each zirconia sample with 0.5 M H_2SO_4 (20 mL) for 3 h and drying at 433 K for 16 h (no filtration). Sieve fractions (500–850 μm) were calcined in a flow of dry air (50 mL/min) at 773 K for 3 h (heating/cooling rate: 10 K/min). The catalysts were stored under dry air.

Catalysis. *Gas-Phase trans-Alkylation of Benzene (1) and Diethylbenzene (2).* The gas-phase trans-alkylation reaction was performed in an automated micro-flow apparatus containing a quartz fixed-bed reactor (i.d. 10 mm) at 10^5 Pa [16 vol % benzene (1 p.a., dried on molsieve), 3.2 vol % diethylbenzene (2, consisting of 25% ortho, 73% meta, and 2% para isomers, dried on molsieve), N_2 balance (50 mL/min), WHSV = 1.5 h^{-1}] with 2.0 mL of the tube reactor filled with catalyst particles (500–850 μm sieve fraction, typically 1.4 g). Two saturators were connected to the inlet of the reactor for the supply of 1 and 2. The partial vapor pressure of 1 and 2 was controlled by adjusting the temperature of the saturator–condensers and the N_2 flow rate. After equilibration for 30 min at the applied reaction temperatures (473 and 673 K, heating rate 10 K/min) within a dry N_2 flow (50 mL/min), benzene (1) and diethylbenzene (2) were passed through the reactor. To prevent condensation of reactants and products prior to GC analysis [Hewlett Packard 5710 A, column: CP-sil 5CB capillary liquid-phase siloxane polymer (100% methyl) 25 m \times 0.25 mm, 323 K, carrier gas: N_2 , FID, sample-loop volume: 1.01 μL], tubes were heat-traced (398 K). FID sensitivity factors and retention times were determined using ethene (99.5%, dried over molsieve) and standard solutions of 1, 2, and ethylbenzene (3, 99%) in methanol (p.a.). The conversion of the feed (compounds 1 and 2) was determined using eq A2 (see the Supporting Information). Notice that the conversion of the feed (compounds 1 and 2) is about 6 times lower than the (partial) conversion of diethylbenzene (2) due to the molar ratio 5:1 of benzene (1) and diethylbenzene (2).

Liquid-Phase Hydro-Acyloxy-Addition of Acetic Acid (4) to Camphene (5). A mixture of glacial acetic acid (4 p.a., 0.70 mol), camphene (5, 95%, 0.70 mol) and acetic anhydride (p.a., 9.05 mmol) was mechanically stirred (1500 rpm) overnight at 328 K under a N_2 atmosphere. Subsequently, 2.5 g of catalyst was quickly suspended in the reaction mixture. The composition of the soluble fraction of the reaction mixture was analyzed by capillary GC as a function of reaction time; samples were prepared as follows: 1.00 mL of the reaction mixture was added to water (25.00 mL) followed by an extraction with *n*-heptane (25.00 mL). 1.00 mL of the *n*-heptane fraction was diluted with *n*-heptane to 25.00 mL in a volumetric flask. 1.0 μL of the diluted solution was injected into the GC [Varian 3400, column: DB-5 capillary liquid-phase siloxane polymer (5% phenyl, 95% methyl), 30 m \times 0.323 mm, temperature program: 5 min at 333 K, 10 K/min to 553 K, 10 min, carrier gas: N_2 , FID]. In the case of hydro-acyloxy-addition reactions performed in the presence of H_2O , 320 μL (17.78 mmol) H_2O was added instead of acetic anhydride (vide supra). To establish whether leaching occurs, the insoluble catalyst particles were removed from the reaction mixture by filtration with a double-ended glass filter under a dry N_2 atmosphere before equilibrium had established. The composition of the reaction mixture was further measured as a function of time. Since no solid residue was found after evaporation of the reaction mixture to dryness in vacuo, the removal of the solid catalysts particles by filtration was complete.

Results and Discussion

Highly Dispersed Silica-Supported ZrO_2 ; Preparation and Characterization. Because our approach starts with the preparation of highly dispersed ZrO_2 on a nonporous silica support ($\text{ZrO}_2/\text{SiO}_2$), which will subsequently be subjected to gas-phase sulfation reactions, two different aqueous precipitation methods were compared, viz., urea hydrolysis and a pH-static procedure. With both methods, hydroxyl ions are homogeneously generated in a suspension of silica in a solution of a zirconium salt. Deposition–precipitation requires that the silica particles will function as nuclei for (hydrated) ZrO_2 precipitation.⁴¹ An important difference between the urea hydrolysis and the pH-static procedure is the pH range in which precipitation of zirconia species proceeds. With urea hydrolysis, ZrO_2 precipitation occurs at $\text{pH} \sim 2$ –3, whereas under pH-static conditions, precipitation necessarily proceeds at $\text{pH} = 4.5$.⁴² The iso-electric point of silica is at $\text{pH} \sim 2$ –3, which brings about that, at pH levels above 3, silica is negatively charged. Adsorption of zirconyl ions and subsequent nucleation of (hydrated) zirconia species on negatively charged silica present at pH levels above 3 is more likely than at lower pH levels.⁴³ Hence, it can be expected that the pH-static method will lead to a better dispersion of ZrO_2 on the silica surface.

The bulk composition of the $\text{ZrO}_2/\text{SiO}_2$ catalyst precursors prepared according to either the urea hydrolysis or the pH-static method was determined by elemental analyses (ICP-AES Zr and Si). Independent of the applied precipitation procedure, similar bulk compositions were found [$\text{Zr} = 6.9 \text{ wt. } \%$, $\text{Si} = 37 \text{ wt. } \%$, residual wt. % = O], which are in reasonable agreement with the calculated values [$\text{Zr} = 7.4 \text{ wt. } \%$, $\text{Si} = 42 \text{ wt. } \%$, residual wt. % = O].

To establish whether a crystalline phase of ZrO_2 has formed within the calcined $\text{ZrO}_2/\text{SiO}_2$ catalyst precursors and to obtain an estimate of the average crystallite size, X-ray diffraction (XRD) was employed. The $\text{ZrO}_2/\text{SiO}_2$ precursors prepared by the urea hydrolysis or the pH-static procedure only showed a background halo due to X-ray scattering of the amorphous silica support (see the Supporting Information, Figure A3).⁴⁴ Hence, the deposited ZrO_2 particles are amorphous. The calcined $\text{ZrO}_2/\text{SiO}_2$ precursors were subsequently studied by transmission electron microscopy (TEM). Despite their similar bulk compositions, TEM shows that the pH-static method leads to supported ZrO_2 particles that are decisively smaller (better dispersion on the silica spheres) than those prepared by urea hydrolysis (Figure 1).

X-ray photoelectron spectroscopy (XPS) was used to assess global differences in the surface composition of the calcined $\text{ZrO}_2/\text{SiO}_2$ catalyst precursors. The $\text{Zr}(3d_{5/2,3/2})/\text{Si}(2s)$ ³⁷ peak-area ratio is the highest for samples prepared by the pH-static precipitation method: $\text{Zr}(3d_{5/2,3/2})/\text{Si}(2s)_{\text{pH-static}} = 2.5$ vs $\text{Zr}(3d_{5/2,3/2})/\text{Si}(2s)_{\text{urea}} = 0.7$ (Figure 2a). Because the bulk compositions of the precursors prepared by the pH-static precipitation method and by urea hydrolysis are identical, the XPS results also indicate that the pH-static precipitation method leads to a higher dispersion of ZrO_2 over the silica surface. Thus, TEM and XPS confirm the conclusion that the interaction between the suspended silica support and the precipitating zirconia species depends on the pH. The availability of more nucleation sites during deposition–precipitation will lead to a metal oxide more highly dispersed on the surface of the silica support. By adjusting the pH, the dispersion of the ZrO_2 can be consequently controlled.

Because the gas-phase sulfation reactions are expected to be more effective for smaller ZrO_2 particles, the $\text{ZrO}_2/\text{SiO}_2$ catalyst

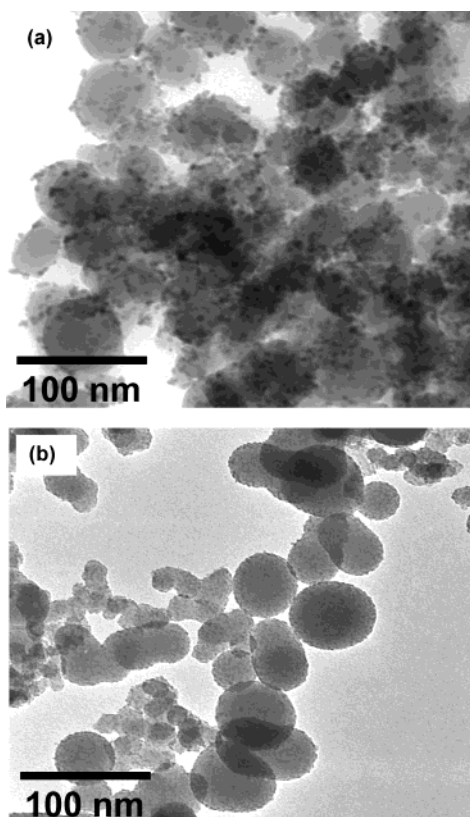


Figure 1. TEM photographs of 10 wt % ZrO₂/SiO₂ prepared by (a) urea hydrolysis and (b) the pH-static method. Large light-gray spheres: silica (Aerosil OX50) support material. Dark dots: metal oxide clusters.

precursors prepared by the pH-static precipitation procedure were used for the gas-phase treatments.

Characterization of Gas-Phase Sulfated ZrO₂/SiO₂. XRD, IR, XPS, and TEM-EDAX were used to evaluate the effectiveness of the three different gas-phase sulfation procedures (H₂S/O₂, SO₂/O₂, and SO₃/SO₂/O₂, see the Experimental Section). After gas-phase sulfation, no changes were detected in the XRD pattern of the ZrO₂/SiO₂ catalysts. Unfortunately, diffuse-reflectance FT-IR is unsuitable to verify the formation of surface sulfides and sulfates due to the interference of the intense Si–O absorption bands. XPS analysis, however, provided more information. Using XPS atomic sensitivity factors [$S(2p) = 0.54$ and $Zr(3d_{5/2,3/2}) = 2.1$]⁴⁵ and the experimental $S(2p)/Zr(3d_{5/2,3/2})$ peak-area ratio, surface atom ratios can be calculated. For bulk anhydrous Zr(SO₄)₂ (prepared from ZrCl₄ and fuming H₂SO₄/10% SO₃),⁶ an $S(2p)/Zr(3d_{5/2,3/2})$ peak-area ratio of 0.50 was previously found,³⁷ which leads to an S/Zr atom ratio of 2.0 in line with the chemical composition. Figure 2b shows the XPS spectra of the ZrO₂/SiO₂ and the gas-treated ZrO₂/SiO₂ catalysts. Gas-phase treatment using H₂S/O₂ led to a $S(2p)$ peak of low intensity positioned at 170.0 eV. For the ZrO₂/SiO₂ catalysts that were subjected to either SO₂/O₂ or SO₃/SO₂/O₂, gas-phase sulfation $S(2p)$ binding energies of 170.0 eV were found, which are in good agreement with the $S(2p)$ binding energy of anhydrous bulk Zr(SO₄)₂ [170.3 eV, see the Supporting Information (Table A1^{6,45–50})]. These results indicate that (partial) conversion of the surface layer of ZrO₂ into Zr(SO₄)₂ has indeed occurred. This is further substantiated by the concomitant shift of the $Zr(3d_{5/2,3/2})$ binding energy from 183.3 eV (blank) to 184.1 eV [SO₃/ZrO₂/SiO₂ (Figure 2b)].³⁷ For bulk anhydrous Zr(SO₄)₂, however, a $Zr(3d_{5/2,3/2})$ binding energy of 185.6 eV was found. The lower $Zr(3d_{5/2,3/2})$ binding energy for

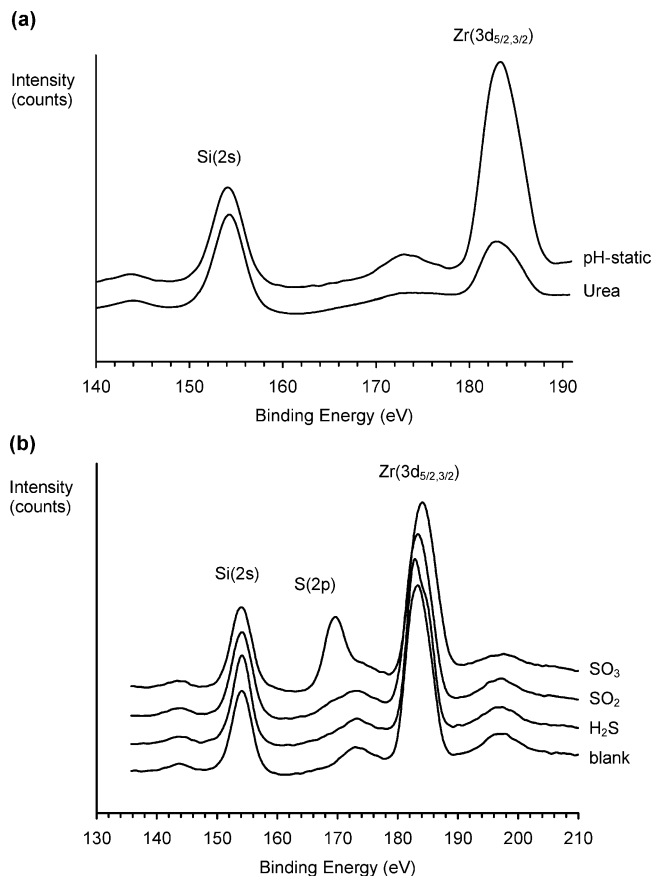


Figure 2. (a) XPS spectra of 10 wt % ZrO₂/SiO₂ prepared by the pH-static method (highest Zr/Si ratio) and urea hydrolysis (lowest Zr/Si ratio). (b) XPS spectra of 10 wt % ZrO₂/SiO₂ (blank) and 10 wt % ZrO₂/SiO₂ subjected to either the H₂S/O₂, SO₂/O₂, or SO₃/SO₂/O₂ gas-phase approach. [The spectra have been corrected for charging, scaled on the Si(2s) peak and vertically displaced for presentation.]

the SO₃/SO₂/O₂-treated ZrO₂/SiO₂ precursor (184.1 eV) in combination with the observed additional broadening of the $Zr(3d_{5/2,3/2})$ peak (0.3 eV $\Delta FWHM$) indicates that both ZrO₂ and Zr(SO₄)₂ are present within the surface layer. This is corroborated by the $S(2p)/Zr(3d_{5/2,3/2})$ peak-area ratio, which was found to be 0.25 (SO₃/SO₂/O₂ treatment) instead of 0.50, which was found for bulk anhydrous Zr(SO₄)₂.⁶

For the conventional, calcined H₂SO₄-impregnated ZrO₂ catalysts (H₂SO₄/ZrO₂), a $S(2p)$ binding energy of 169.3 eV has been reported, which deviates significantly from the $S(2p)$ binding energy of bulk anhydrous Zr(SO₄)₂ (170.3 eV).^{6,18,51} Interestingly, the $S(2p)$ binding energy in H₂SO₄/ZrO₂ is nearly identical to that of liquid H₂SO₄ (169.4 eV, see also the Supporting Information Table A1). In addition, the $Zr(3d_{5/2,3/2})$ binding energy of the H₂SO₄/ZrO₂ catalysts is mainly determined by the contribution of ZrO₂, especially after calcination at high temperatures (923 K).^{18,24} For H₂SO₄/ZrO₂ catalysts calcined at lower temperatures (773 K), a broadened $Zr(3d_{5/2,3/2})$ peak is found, which was ascribed to the presence of primarily ZrO₂ within the surface layer.^{24,43} Note that the impregnated zirconia's used in the catalytic experiments were calcined at 773 K. Deconvolution of the broadened $Zr(3d_{5/2,3/2})$ peak resulted in $Zr(3d_{5/2})$ and $Zr(3d_{3/2})$ binding energies still lower than the $Zr(3d_{5/2})$ and $Zr(3d_{3/2})$ binding energies of Zr(SO₄)₂·4H₂O (184.5 and 186.5 eV, respectively).^{18,24} Hence, calcination at 773 K of conventionally prepared, H₂SO₄-impregnated/ZrO₂ catalysts and subsequent exposure to ambient air apparently does not result in the presence of either Zr(SO₄)₂·4H₂O or Zr(SO₄)₂ within the surface layer.

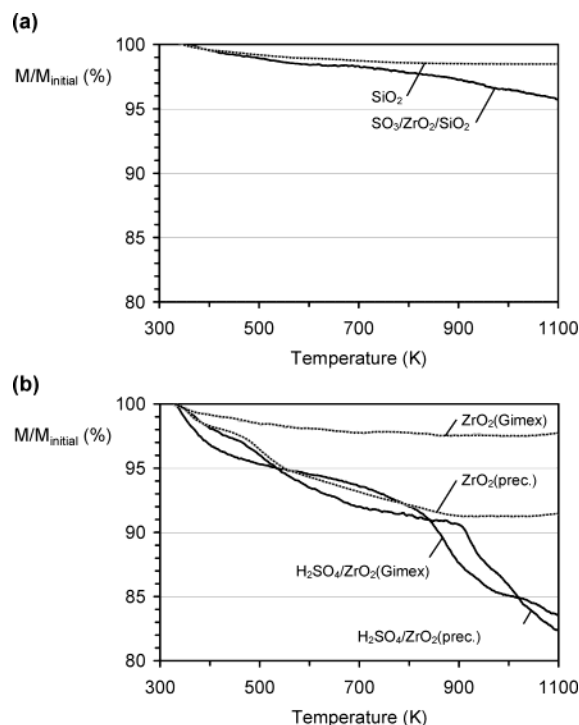


Figure 3. Thermogravimetric analysis of (a) SiO_2 and $\text{SO}_3/\text{ZrO}_2/\text{SiO}_2$ and (b) $\text{ZrO}_2(\text{Gimex})$ and $\text{ZrO}_2(\text{prec.})$ and corresponding (calcined) H_2SO_4 -impregnated catalysts. [Temperature program: 30 min at 323 K, 10 K/min to 1100 K and 10 min at 1100 K.]

TABLE 1: ICP-AES and Flash-Combustion GC Results for the 10 wt % $\text{ZrO}_2/\text{SiO}_2$ Catalyst Precursor Materials Subjected to the Gas-Phase $\text{SO}_3/\text{SO}_2/\text{O}_2$ Treatment and for the Two Conventional $\text{H}_2\text{SO}_4/\text{ZrO}_2$ Catalyst Materials^a

sample	element	atom (%)		BET area (m^2/g)
		calc. (100% sulfated)	ICP-AES/flash-combustion GC	
$\text{SO}_3/\text{ZrO}_2/\text{SiO}_2$	S	3.0	1.7	50
	Zr	1.5	1.3	
	Si	27.6	23.7	
$\text{H}_2\text{SO}_4/\text{ZrO}_2(\text{prec.})$	S	7.3	4.0	217
	Zr	23.9	23.9	
$\text{H}_2\text{SO}_4/\text{ZrO}_2(\text{Gimex})$	S	7.3	1.8	50
	Zr	23.9	24.2	

^a Residual atom (%): oxygen.

With TEM-EDAX, it was established that the initial dispersion of ZrO_2 on the silica support (Figure 1) did not change during the subsequent gas treatments. This result is in line with the near constant XPS $\text{Zr}(3d_{5/2,3/2})/\text{Si}(2s)$ peak intensity ratio found (Figure 2b). The results furthermore show that the $\text{SO}_3/\text{SO}_2/\text{O}_2$ treatment (Chart 1; reaction 3) appears to be the most effective for the preparation of highly dispersed silica-supported zirconium sulfates. Therefore, this gas-phase sulfated catalyst was further characterized and its catalytic properties were evaluated.

Table 1 presents the results of the elemental analyses as well as the specific surface areas (BET method) of the $\text{SO}_3/\text{ZrO}_2/\text{SiO}_2$ catalyst and the two sulfated zirconia catalysts. The results show that the amount of sulfur (at. %) and the specific surface area are higher for the sulfated zirconia ($\text{H}_2\text{SO}_4/\text{ZrO}_2$) prepared from freshly precipitated zirconia than for that prepared from the Gimex zirconia and the $\text{SO}_3/\text{ZrO}_2/\text{SiO}_2$ catalyst (Table 1).⁵² However, the amount of sulfur per unit surface area is larger for the sulfated zirconia prepared from Gimex zirconia. Fur-

thermore, the sulfur-to-zirconium ratio is much higher for the supported catalyst, as has to be expected.

Thermal Stability of $\text{SO}_3/\text{ZrO}_2/\text{SiO}_2$ and $\text{H}_2\text{SO}_4/\text{ZrO}_2$. An important distinction between the $\text{SO}_3/\text{ZrO}_2/\text{SiO}_2$ catalysts (prepared via the gas-phase procedure) and the water-free bulk zirconium sulfate, on one hand, and the usual sulfated zirconia catalysts ($\text{H}_2\text{SO}_4/\text{ZrO}_2$; conventionally prepared by impregnation with H_2SO_4), on the other hand, is the presence of H_2SO_4 . The XPS results point to sulfuric acid in the surface layer of the sulfated zirconia's. Sulfuric acid can be present due to an incomplete reaction with the surface of the impregnated zirconia or hydrolysis of zirconium sulfate by residual water or water from ambient air. Anhydrous bulk $\text{Zr}(\text{SO}_4)_2$ exhibits an onset temperature of decomposition in a dry N_2 flow of 890 K,⁶ while the constituents of sulfuric acid are significantly present in the gas-phase already above a temperature of 473 K (see the Supporting Information; Figure A4^{53–56}). Figure A4 indicates that, for compositions of a mol fraction of SO_3 below 0.5 (diluted H_2SO_4) at temperatures below 473 K, only water will be released into the gas flow.⁵⁷ Hence, heating from room temperature will cause water to evaporate and, consequently, lead to an increase in concentration of the H_2SO_4 . Above 473 K, however, also significant amounts of the constituents of H_2SO_4 will be present in the gas phase. Sulfuric acid present in the catalysts, consequently, will be apparent from a loss in weight at temperatures appreciably lower than 890 K. The $\text{SO}_3/\text{ZrO}_2/\text{SiO}_2$ and the sulfated zirconia ($\text{H}_2\text{SO}_4/\text{ZrO}_2$) catalysts were therefore subjected to thermogravimetric analysis. The thermal stability of the sulfated metal oxide catalysts will furthermore indicate the temperature range in which the catalysts can be expected to remain catalytically active.

The thermal stability of silica and (nonsulfated) zirconia was measured by TGA (N_2) (Figure 3). Whereas the silica support and $\text{ZrO}_2(\text{Gimex})$ only eliminated a minute amount of water, the water content of the $\text{ZrO}_2(\text{prec.})$ is appreciably higher as is evident from the relatively large decrease in weight. Figure 3 also represents the weight loss of the $\text{SO}_3/\text{ZrO}_2/\text{SiO}_2$ and sulfated zirconia ($\text{H}_2\text{SO}_4/\text{ZrO}_2$) catalysts, which was also measured in a flow of nitrogen. The $\text{SO}_3/\text{ZrO}_2/\text{SiO}_2$ catalyst exhibited a small continuous decrease in weight (Figure 3a). Decomposition of the sulfate smoothly follows the loss of water, which proceeds at low temperatures. Elimination of water from the $\text{SO}_3/\text{ZrO}_2/\text{SiO}_2$ catalysts must originate from the silica support, because the XPS results did not indicate the presence of H_2SO_4 (vide supra). However, the thermal stability of $\text{Zr}(\text{SO}_4)_2$ in the presence of water vapor is much lower.⁶ Hence, for the $\text{SO}_3/\text{ZrO}_2/\text{SiO}_2$ catalyst materials, formation of a small amount of H_2SO_4 or bisulfate groups ($-\text{OSO}_3\text{H}$) by reaction with water from the silica support cannot be excluded.

The conventional sulfated zirconia ($\text{H}_2\text{SO}_4/\text{ZrO}_2$) catalysts showed a much larger weight loss (Figure 3b). The TGA curves for the zirconia's and the $\text{H}_2\text{SO}_4/\text{ZrO}_2$ catalysts are identical to those previously published.²⁴ Figure 3 shows that a continuous decrease in weight sets on below 373 K. The initial weight loss is attributed to the removal of water. It is interesting that the curves for precipitated zirconia and the sulfated precipitated zirconia run parallel up to a temperature of about 530 K. Up to 530 K, desorption of water from the sulfated precipitated zirconia is consequently likely. At higher temperatures the weight loss of the sulfated zirconia (H_2SO_4) is slightly higher. Above 530 K, the sulfated zirconia's ($\text{H}_2\text{SO}_4/\text{ZrO}_2$) can release water from grafted H_2SO_4 or bisulfate groups ($-\text{OSO}_3\text{H}$), but also the constituents of sulfuric acid will be volatilized.^{6,8,9,24} The catalyst prepared from the Gimex zirconia showed a steep

TABLE 2: Elemental Analysis (S/Si Atom Ratio) by ICP-AES and Flash-Combustion GC (Global Bulk Composition), XPS (Global Surface Composition), and SEM-EDAX (Local Bulk Composition) of SO₃/ZrO₂/SiO₂, after Treatment with H₂O_(g) at 473 and 673 K for 10 h Followed by Resuspension in H₂O_(l) (293 K, 1 h)

treatment of SO ₃ /ZrO ₂ /SiO ₂	S/Si (atom ratio)		
	flash- combustion GC & ICP-AES	XPS	SEM-EDAX multiple point analysis, 20-point average
H ₂ O _(g) , 473 K	0.072	0.22	0.024
H ₂ O _(g) , 673 K	0.073	0.18	0.019
H ₂ O _(g) , 673 K	0.059	0.06	0.008
H ₂ O _(l) , 293 K	0.029	0.05	0.006

weight loss setting on at about 800 K and that prepared from the precipitated zirconia only above about 910 K. The weight loss at about 890 K for the H₂SO₄/ZrO₂ catalysts (Figure 3b) and the SO₃/ZrO₂/SiO₂ catalyst (Figure 3a) is also observed for bulk anhydrous Zr(SO₄)₂ (within a dry N₂ flow).⁶ The steep weight loss indicates that Zr(SO₄)₂ has been formed in the sulfated zirconia (H₂SO₄/ZrO₂) catalysts. The zirconium sulfate can be present at temperatures up to about 530 K underneath a layer of sulfuric acid. The sulfuric acid has desorbed at the temperature of the steep weight loss. The sulfuric acid may have remained after the impregnation, drying, and calcinations for 3 h at 773 K. However, the surface of the sulfated zirconia is highly hygroscopic. Water taken up during transport and storage may hydrolyze the zirconium sulfate of the surface layer to sulfuric acid and zirconia; this has to be prevented.

The TGA curves of Figure 3 also reflect a pronounced difference in the macroscopic structure (porosity) of the sulfated zirconia (H₂SO₄/ZrO₂) catalysts. A comparison of the curves of the two catalysts, viz., H₂SO₄/ZrO₂(prec.) and H₂SO₄/ZrO₂-(Gimex), reveals that the elimination of water, the release of the constituents of H₂SO₄, and the decomposition of Zr(SO₄)₂ proceeded at higher temperatures with the H₂SO₄/ZrO₂(prec.) catalyst. The surface area of the H₂SO₄/ZrO₂(prec.) catalyst (217 m²/g) is considerably larger than that of the H₂SO₄/ZrO₂(Gimex) catalyst (50 m²/g). Transport of gas molecules interacting significantly with the walls of the pores will proceed much slower out of the more highly porous structure of the H₂SO₄/ZrO₂(prec.) catalyst.

Stability of SO₃/ZrO₂/SiO₂ toward Water Vapor. Additional support for the presence of grafted H₂SO₄ or bisulfate groups (–OSO₃H) in the conventional sulfated zirconia (H₂SO₄/ZrO₂) catalysts comes from FT-IR analyses.^{6,7,20–23} The sulfated zirconia catalysts possess a heterogeneous surface structure, which changes concomitant with temperature, pressure, and/or the presence of water vapor. Above 473 K, dehydration is accompanied by elimination of H₂SO₄ (see the Supporting Information, Figure A4). This implies that hydration can lead to an irreversible loss of sulfate at temperatures above 473 K under flow conditions. Such irreversible behavior was observed for anhydrous bulk Zr(SO₄)₂.^{6,58–62} With sulfated zirconia catalysts being employed at temperatures above 473 K, consequently, elimination of corrosive constituents of sulfuric acid can be expected above 473 K, especially if water vapor is present. Because the active component of the catalysts will then be lost, the activity of the catalysts will drop. Also contact of sulfated zirconia's with a flow of liquid water will lead to a loss of sulfate by hydrolysis and dissolution of the resulting sulfuric acid.

To establish the loss of sulfate experimentally, the SO₃/ZrO₂/SiO₂ catalyst was exposed to a gas flow containing water vapor for 10 h at 473 and 673 K. Table 2 represents the results of

elemental analyses (Flash-combustion GC and ICP-AES, XPS, and SEM-EDAX) of the SO₃/ZrO₂/SiO₂ catalyst before and after prolonged exposure to steam. Comparison of the S/Si atom ratios of the SO₃/ZrO₂/SiO₂ catalyst before and after the steam-treatment consistently indicates that the catalyst previously calcined in dry air at 723 K loses sulfate upon exposure to water vapor at 673 K. The larger drop in sulfate content apparent from the XPS and SEM-EDAX measurements suggests that the external surface layer of the catalyst loses the sulfate more rapidly than the walls of the pores within the catalyst grains. The effect of the rate of transport was also evident in the thermogravimetric experiments. The data of Table 2 suggest that sulfated zirconia catalysts can be employed in gas flows containing steam at temperatures up to about 473 K *without* a rapid loss in activity. Immersion of the catalyst in liquid water of 293 K for 1 h resulted in a large loss of sulfate. In the presence of liquid water, sulfated zirconia therefore is not a solid acid catalyst but produces dissolved sulfuric acid.

Catalytic Activity of Conventional H₂SO₄/ZrO₂ vs SO₃/ZrO₂/SiO₂ in the Gas-Phase trans-Alkylation of Benzene (1) and Diethylbenzene (2). To assess the applicability of our different sulfated zirconia catalysts in gas-phase reactions, the trans-alkylation reaction of benzene (1) and diethylbenzene (2, Chart 2; reaction 4)^{27–30} was studied at 10⁵ Pa in a fixed-bed reactor with a 16 vol % benzene (1) and 3.2 vol % diethylbenzene (2) feed. The conversion of the feed [benzene (1) and diethylbenzene (2, see the Supporting Information, eq A2)] was determined as a function of time. First, the catalytic performance of the sulfated metal oxide catalysts in the gas-phase trans-alkylation reaction of 1 and 2 was benchmarked at 473 and 673 K with an amorphous aluminosilicate (ASA) (Si/Al = 12, BET specific area = 320 m²/g) (Figure 4a). At 673 K, the conversion is about eight times higher than the low conversion at 473 K. The higher conversion at 673 K is not only due to the effect of the higher temperature on the trans-alkylation reaction but also to the (more temperature-dependent) formation of ethene (see the Supporting Information; Figure A5). The ethylbenzene (3) selectivity is 100% at 473 K but only 50% at 673 K. The initial rapid deactivation of the catalyst at 673 K may be due to oligomerization of ethene on the acid sites and subsequent reaction to carbonaceous deposits.

Figure 4, parts b and c, represents the conversion of 1 and 2 at 473 and 673 K in the presence of the conventionally prepared sulfated zirconia (H₂SO₄/ZrO₂) catalysts. The H₂SO₄/ZrO₂-(Gimex) exhibited a negligible activity at 673 K and initially a significant activity at 473 K (Figure 4c). However, the activity dropped, and after 300 min, the activity was negligible. The activity of the H₂SO₄/ZrO₂(prec.) catalyst was at 473 K considerable and stable (Figure 4b). In contrast to the behavior of the reference ASA catalyst, the activity at 673 K of the H₂SO₄/ZrO₂(prec.) catalyst was much lower. When after the reaction at 673 K the H₂SO₄/ZrO₂(prec.) catalyst was cooled to 473 K, the activity appeared to be completely lost; the conversion was not significant.

Figure 4d shows the activity of the SO₃/ZrO₂/SiO₂ catalyst at 473 K. It can be seen that the initial activity disappears within 80 min. To demonstrate that the initial activity is due to the uptake of water during transport from ambient air, the catalyst was exposed for 2 h to a flow of 50 mL/min of nitrogen containing 2 vol % of water vapor at 473 K. From Figure 4d, it can be seen that the activity of the catalyst exposed to water vapor is higher and more stable. The activity now disappears within about 350 min. The activity of the anhydrous bulk Zr(SO₄)₂ is represented in Figure 4e, which indicates that the

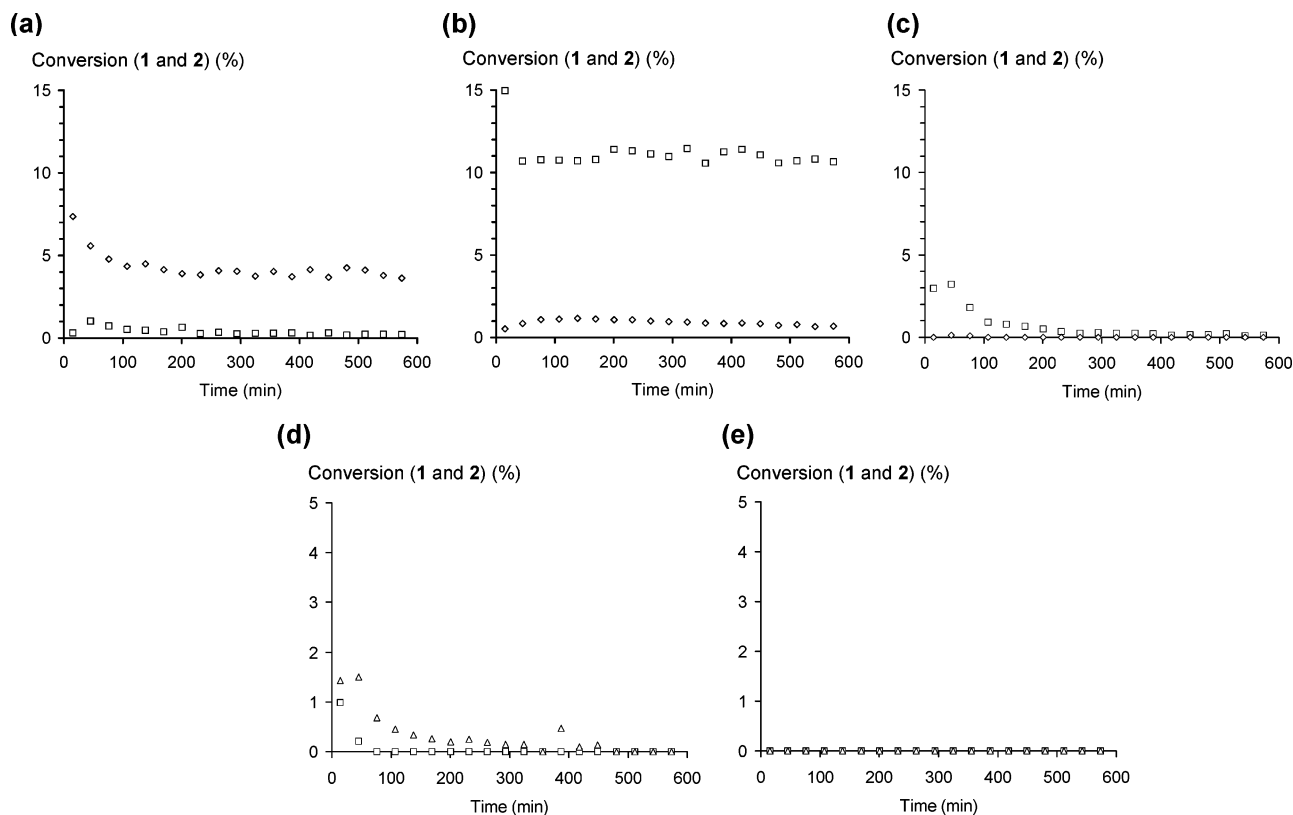


Figure 4. Conversion in the trans-alkylation of benzene (1) and diethylbenzene (2) with (a) ASA, (b) $\text{H}_2\text{SO}_4/\text{ZrO}_2(\text{prec.})$, and (c) $\text{H}_2\text{SO}_4/\text{ZrO}_2(\text{Gimex})$; \square 473 K and \diamond 673 K. Conversion in the trans-alkylation of benzene (1) and diethylbenzene (2) at 473 K with (d) $\text{SO}_3/\text{ZrO}_2/\text{SiO}_2$ and (e) bulk anhydrous $\text{Zr}(\text{SO}_4)_2$; \square not hydrated and \triangle hydrated (2 h, 2% H_2O , 50 mL/min). [Conversion of the feed (compounds 1 and 2) gives values that are about 6 times lower than the (partial) conversion of diethylbenzene (2) because the molar ratio benzene (1):diethylbenzene (2) is 5:1.]

anhydrous sulfate has no any catalytic activity in the gas-phase trans-alkylation reaction of benzene (1) and diethylbenzene (2). Accordingly, Lewis acid sites catalyzing the trans-alkylation are not available in water-free bulk zirconium sulfate. In contrast to the $\text{SO}_3/\text{ZrO}_2/\text{SiO}_2$ catalyst, prehydration of anhydrous bulk $\text{Zr}(\text{SO}_4)_2$ with an *sub*-stoichiometric quantity of water vapor did not lead to a significant conversion. That no catalytic activity is induced with the water-free bulk sulfate is due to the formation of a rather stable tetrahydrate $[\text{Zr}(\text{SO}_4)_2 \cdot 4\text{H}_2\text{O}]$, which suppresses the hydrolysis reaction of anhydrous bulk $\text{Zr}(\text{SO}_4)_2$.⁶

The fact that water vapor is required to activate the silica-supported water-free zirconium sulfate catalyst is in line with H_2SO_4 to be the catalytically active species within $\text{H}_2\text{SO}_4/\text{ZrO}_2$ catalysts. After calcinations for 3 h at 773 K, the $\text{H}_2\text{SO}_4/\text{ZrO}_2(\text{Gimex})$ catalyst has lost the water and sulfuric acid almost completely leaving behind a surface layer containing zirconium sulfate. During transport and loading into the reactor, the catalyst takes up water, which will react with the surface of the zirconium sulfate to zirconium bisulfate and sulfuric acid. At 473 K, it takes about 300 min for the water to evaporate, which leaves an inactive zirconium sulfate surface. The release of water and the constituents of sulfuric acid from the relatively open structure of the $\text{H}_2\text{SO}_4/\text{ZrO}_2(\text{Gimex})$ catalyst proceeds so rapidly at 673 K that no measurable activity is exhibited. Calcination for 3 h at 773 K is not sufficient to remove the sulfuric acid and some water completely out of the highly porous structure of the $\text{H}_2\text{SO}_4/\text{ZrO}_2(\text{prec.})$ catalyst. Accordingly, the catalyst exhibits a substantial activity at 473 K (Figure 4b). Keeping the $\text{H}_2\text{SO}_4/\text{ZrO}_2(\text{prec.})$ catalyst in a gas flow at 673 K rapidly removes the water and the constituents of sulfuric acid from the easily accessible sites within the catalyst structure. The remaining activity is consequently low. Subsequent measurement of the activity at 473 K results in a negligible activity,

because the sulfuric acid has been removed from the sites that are most readily accessible from the gas phase.

The above results indicate that water is required for $\text{H}_2\text{SO}_4/\text{ZrO}_2$ and $\text{SO}_3/\text{ZrO}_2/\text{SiO}_2$ catalysts to be catalytically active. H_2SO_4 is not released below 473 K in a gas flow and will remain on the surface of the catalyst (see the Supporting Information Figure A4 and Table 2). Nevertheless, the $\text{H}_2\text{SO}_4/\text{ZrO}_2(\text{Gimex})$ catalyst lost the activity within 300 min at 473 K and the $\text{SO}_3/\text{ZrO}_2/\text{SiO}_2$ catalyst within 80 min. Consequently, water can only be released in the gas flow, which proves that water is required to activate sulfuric acid present on the surface of the catalysts. Presumably, water is required to shift the equilibrium of the hydrolysis of zirconium sulfate to the zirconium oxide and sulfuric acid side. When water is removed, the equilibrium shifts to the inactive zirconium sulfate side.

In liquid-phase reactions, contact with liquid water may lead to dissolution of sulfuric acid, which becomes subsequently active as a homogeneous catalyst. The difference in catalytic activity between the $\text{H}_2\text{SO}_4/\text{ZrO}_2(\text{prec.})$ and the $\text{H}_2\text{SO}_4/\text{ZrO}_2(\text{Gimex})$ catalyst in the gas-phase trans-alkylation was attributed to a difference in the rate of transport through the porous structure of the catalysts. Because transport within liquids is much slower than that within the gas phase, a different rate of transport will also affect the apparent activity in the liquid phase. The above prompted us to study the $\text{H}_2\text{SO}_4/\text{ZrO}_2$ and $\text{SO}_3/\text{ZrO}_2/\text{SiO}_2$ catalysts in a liquid-phase reaction.

Stability of $\text{SO}_3/\text{ZrO}_2/\text{SiO}_2$ and $\text{H}_2\text{SO}_4/\text{ZrO}_2$ toward Liquid Water. Table 2 also mentions the effect of the contact with liquid water on the sulfate content of the $\text{SO}_3/\text{ZrO}_2/\text{SiO}_2$ catalyst. After stirring the $\text{SO}_3/\text{ZrO}_2/\text{SiO}_2$ catalyst in water for 1 h, followed by filtration and drying (393 K), elemental analysis (flash-combustion GC and ICP-AES, XPS, and SEM-EDAX) revealed that the S/Si atom ratio decreases by a factor of 2.45

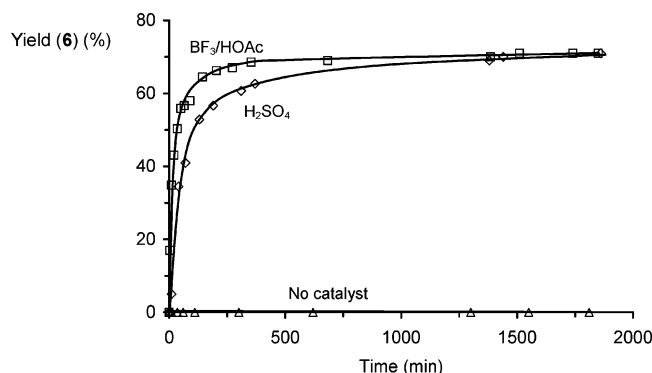


Figure 5. Formation of isobornyl acetate (**6**) for the hydro-acyloxy-addition of 0.70 mol glacial acetic acid (**4**) to 0.70 mol camphene (**5**) at 338 K (stirred tank-reactor, N₂ atmosphere); Δ no catalyst, \square 8.75 mmol of BF₃/HOAc, and \diamond 1.65 mL of 5.3 M H₂SO₄.

(Table 2). In addition, the filtrates from aqueous suspensions of the SO₃/ZrO₂/SiO₂ and H₂SO₄/ZrO₂ were all found to have a pH of about 1–2. Therefore, it can be concluded that in the presence of liquid water leaching of H₂SO₄ from these catalysts occurs. If H₂SO₄ is either present on the catalyst or is generated via hydrolysis, it will thus dissolve into the reaction mixture provided sulfuric acid is soluble in the liquid and act as a homogeneous acid catalyst.

Catalytic Activity of H₂SO₄/ZrO₂ and SO₃/ZrO₂/SiO₂ in Liquid-Phase Reactions. To assess the catalytic performance of H₂SO₄/ZrO₂ and SO₃/ZrO₂/SiO₂ in the liquid-phase, the liquid-phase hydro-acyloxy-addition reaction of acetic acid (**4**) to camphene (**5**) giving the industrial important pine-fragrance isobornyl acetate (**6**, Chart 2; reaction 5)^{2,27,31–34} was chosen, in which water is neither formed nor present. The presence of a strong acid as catalyst, such as BF₃/HOAc or H₂SO₄, is required to establish the equilibrium corresponding to the reaction. Under the employed conditions, 70% of **6** can be formed (Figure 5, see the Experimental Section).

Anhydrous Zr(SO₄)₂ was found to be catalytically inactive in the hydro-acyloxy-addition reaction.⁶ In analogy with the gas-phase trans-alkylation reaction of benzene (**1**) and diethylbenzene (**2**, Figure 4e), this shows that anhydrous Zr(SO₄)₂ is not catalytically active as a Lewis acid. With the sulfated zirconia (H₂SO₄/ZrO₂) catalysts, however, isobornyl acetate (**6**) was immediately formed (Figure 6a). Removal of the solid catalyst particles from the reaction mixture by filtration (see the Experimental Section) did not stop the formation of **6**, albeit a decrease in reaction rate was observed. Hence, it appears that H₂SO₄ slowly dissolves from the zirconia into the reaction mixture and acts as a homogeneous catalyst. Although the sulfur content of the H₂SO₄/ZrO₂(prec.) catalyst is higher than that of the H₂SO₄/ZrO₂(Gimex) catalyst (Table 1), the rate of formation of **6** is lower with the H₂SO₄/ZrO₂(prec.) catalyst. The lower activity of the H₂SO₄/ZrO₂(prec.) catalyst indicates that leaching of H₂SO₄ and/or the accessibility of the catalytically active groups is less for the highly porous H₂SO₄/ZrO₂(prec.) catalyst than for the less porous H₂SO₄/ZrO₂(Gimex) catalyst. The lower porosity of the ZrO₂(Gimex) brings about that calcination leads to a loss of H₂SO₄, which is much more rapid than that of the much more porous precipitated ZrO₂(prec.). Within the liquid phase, the transport through the highly porous H₂SO₄/ZrO₂(prec.) catalyst is, however, much slower. Consequently, the more accessible H₂SO₄ within the ZrO₂(Gimex) is more active and dissolves faster.

With the SO₃/ZrO₂/SiO₂ catalysts, addition of water to the reaction mixture was a prerequisite to observe activity (Figure

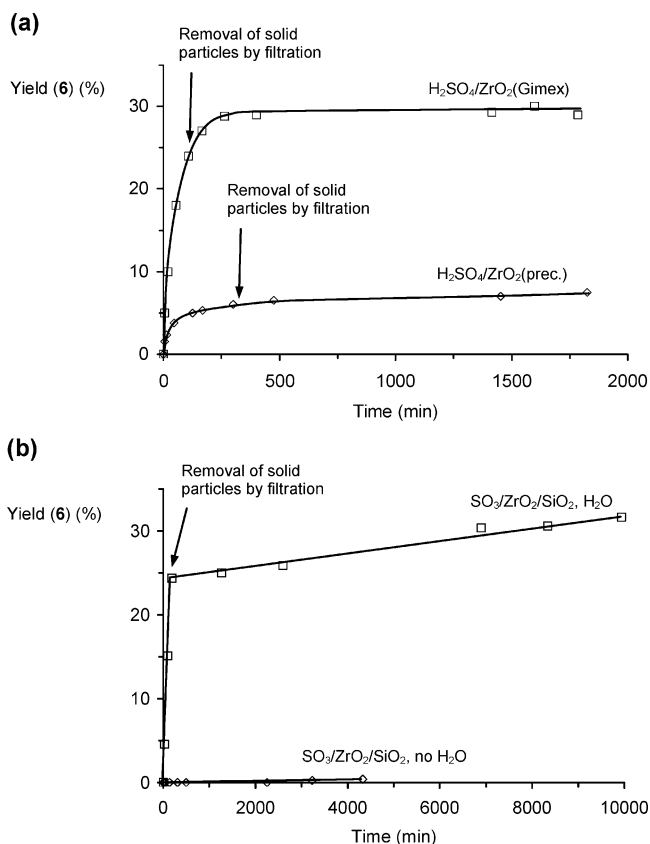


Figure 6. Formation of isobornyl acetate (**6**) by the hydro-acyloxy-addition of 0.70 mol glacial acetic acid (**4**) to 0.70 mol camphene (**5**) at 338 K (stirred tank-reactor, N₂ atmosphere); (a) \square 2.5 g of H₂SO₄/ZrO₂(Gimex) without H₂O, \diamond 2.5 g of H₂SO₄/ZrO₂(prec.) without H₂O; (b) \diamond 2.5 g of SO₃/ZrO₂/SiO₂ without H₂O, \square 2.5 g of SO₃/ZrO₂/SiO₂ and 320 μ L (17.78 mmol) H₂O.

6b). The presence of water was also necessary to obtain isobornyl acetate (**6**) with anhydrous Zr(SO₄)₂.⁶ Hence, no Lewis acid type catalytic activity is observed with the SO₃/ZrO₂/SiO₂ catalysts. It is important to note that in the gas-phase reaction a sub-stoichiometric quantity of water was introduced, whereas a much larger amount of water was added in the liquid-phase reaction. After removal of the SO₃/ZrO₂/SiO₂ particles from the reaction mixture (with extra water present) by filtration, the formation of **6** did not stop. Nonetheless, the reaction rate decreased (Figure 6b). In analogy with the sulfated zirconia (H₂SO₄/ZrO₂) catalysts, H₂SO₄ slowly dissolves from the surface of the SO₃/ZrO₂/SiO₂ catalysts into the reaction mixture and subsequently homogeneously catalyzes the reaction. Because the H₂SO₄/ZrO₂ and SO₃/ZrO₂/SiO₂ catalysts are susceptible to hydrolysis and leaching of catalytically active, but corrosive H₂SO₄, it can be questioned whether these catalysts are that benign as frequently proposed.^{1,3–5}

Conclusions

This research has substantiated that the activity of sulfated zirconia is governed by the equilibria: $\text{Zr(SO}_4)_2 + 4\text{H}_2\text{O} \rightleftharpoons \text{Zr(SO}_4)_2 \cdot 4\text{H}_2\text{O} + n\text{H}_2\text{O} \rightleftharpoons \text{ZrO}_2 + 2\text{H}_2\text{SO}_4\text{aq}$.

For the thermal pretreatment of sulfated zirconia, it is important that the constituents of sulfuric acid exhibit a considerable vapor pressure at significantly lower temperatures than the temperatures at which zirconium sulfate decomposes. The rate of transport of water out of a catalyst batch being thermally pretreated is therefore decisive for the final activity of the catalyst. Rapid release of water leads to water-free

zirconium sulfate, which is only active as a solid acid catalyst after exposure to an amount of water vapor sufficient to exceed the amount required for the reaction to the tetrahydrate. Because water vapor strongly adsorbs on the surface of zirconia and sulfated zirconia, the transport of water out of porous zirconia's and out of large catalyst batches will proceed slowly. Consequently, the final catalyst will have retained a sufficiently large fraction of water to provide a highly active catalyst. However, keeping a catalyst for a long period of time in a gas flow containing water vapor at a sufficiently elevated temperature can lead to a substantial loss of sulfate. Consequently, the material situated at the external edge of a larger catalyst batch can appreciably lose sulfate.

The volatility of the components of the active species also affects the activity in gas-phase reactions. At temperatures above about 473 K, both water and sulfuric acid can volatilize. When water is added to the reactants, the hydrolysis of zirconium sulfate can continue and the catalyst can slowly deactivate irreversibly. Utilization of sulfated zirconia catalysts in gas-phase reactions at temperatures significantly above about 473 K will therefore presumably not lead to a catalyst displaying a stable performance during low periods of time. At lower temperatures only, the release of water has to be envisioned, which also leads to an inactive catalyst. Addition of some steam to the reactants therefore may be required to maintain the activity at a constant, high level at temperatures below about 473 K.

Sulfated zirconia is a particularly interesting catalyst in liquid-phase reactions. Activity calls for the above equilibria being situated at the right-hand side. Sufficiently hydrated sulfated zirconia's can exhibit excellent catalytic properties in liquid-phase reactions, provided the solubility of sulfuric acid in the reaction medium is negligible.

In the gas-phase trans-alkylation reaction, the sulfated metal oxide catalysts showed a lower conversion of diethylbenzene (2) at 673 K than at 473 K, which is in contrast to the catalytic performance of a conventional acid amorphous aluminum silicate catalyst. According to elemental analyses and in line with the temperature-composition diagram of the system H_2O – SO_3 (H_2SO_4), the inverse temperature dependence is a consequence of the loss of catalytically active H_2SO_4 above 473 K. Hence, in gas-phase reactions, these catalysts can only be used below 473 K. In the liquid-phase hydro-acyloxy-addition reaction, supported H_2SO_4 slowly leaches in the reaction mixture and thus provides a homogeneous catalyst. Removal of the solid catalyst particles from the reaction mixture by filtration consequently did not stop the production of isobornyl acetate (6).

The main conclusion of this research is that the catalytic activity of sulfated zirconia catalysts originates from supported sulfuric acid containing water. The deficiencies of water-diluted sulfuric acid, volatility and solubility in liquid, have to be considered in the technical utilization of sulfated zirconia catalysts.

Acknowledgment. This work was carried out as part of the Innovation Oriented Research Program on Catalysis (IOP Katalyse, no. IKA96023b) sponsored by The Netherlands Ministry of Economic Affairs (financial support I.J.D.). Dr. O. L. J. Gijzeman and A.J.M. Mens (Utrecht University, Department of Inorganic Chemistry and Catalysis) are gratefully acknowledged for performing the XPS measurements. B.H. Reesink and R. Ansems (Engelhard De Meern B.V., The Netherlands) kindly performed the ICP-AES and Flash-combustion GC analyses.

Supporting Information Available: Schematic representation of the reactor used for the gas-phase treatments of the silica-supported metal oxides and additional figures, tables, and equations (8 pages). This material is available free of charge via the Internet at <http://pubs.acs.org>.

References and Notes

- (1) Tanabe, K.; Hölderich, W. F. *Appl. Catal. A* **1999**, *181*, 399–434.
- (2) Bledsoe, J. O. Terpenoids. In *Kirk-Othmer Encyclopedia of Chemical Technology*, 4th ed.; Kroschwitz, J. I., Howe-Grant, M., Eds.; Wiley: New York, 1997; Vol. 23, pp 833–882.
- (3) Tanabe, K.; Misono, M.; Ono, Y.; Hattori, H. *New Solid Acids and Bases – Their Catalytic Properties*; Elsevier: Amsterdam, 1989.
- (4) Yadav, G. D.; Nair, J. J. *Microporous Mesoporous Mater.* **1999**, *33*, 1–48.
- (5) Song, X.; Sayari, A. *Catal. Rev. – Sci. Eng.* **1996**, *38*, 329–412.
- (6) Dijks, I. J.; de Koning, R.; Geus, J. W.; Jenneskens, L. W. *Phys. Chem. Chem. Phys.* **2001**, *3*, 4423–4429 and references therein.
- (7) Babou, F.; Coudurier, G.; Vedrine, J. J. *Catal.* **1995**, *152*, 341–349.
- (8) Fărcașiu, D.; Li, J. Q. *Appl. Catal. A* **1998**, *175*, 1–9 and references therein.
- (9) Fraenkel, D. *Ind. Eng. Chem. Res.* **1997**, *36*, 52–59.
- (10) Nagase, Y.; Jin, T.; Hattori, H.; Yamaguchi, T.; Tanabe, K. *Bull. Chem. Soc. Jpn.* **1985**, *58*, 916–918.
- (11) Rack Sohn, J.; Won Kim, H. *J. Mol. Catal.* **1989**, *52*, 361–374.
- (12) Morterra, C.; Cerrato, G.; Di Ciero, S.; Signoretto, M.; Pinna, F.; Strukul, G. *J. Catal.* **1997**, *165*, 172–183.
- (13) Ng, F. T. T.; Horvát, N. *Appl. Catal. A* **1995**, *123*, L197–L203.
- (14) Ebitani, K.; Konno, H.; Tanaka, T.; Hattori, H. *J. Catal.* **1992**, *135*, 60–67.
- (15) Brenner, A. M.; Schrod, J. T.; Shi, B.; Davis, B. H. *Catal. Today* **1998**, *44*, 235–244.
- (16) Jin, T.; Machida, M.; Yamaguchi, T.; Tanabe, K. *Inorg. Chem.* **1984**, *23*, 4396–4398.
- (17) Fărcașiu, D.; Li, J. Q.; Kogelbauer, A. *J. Mol. Catal. A: Chem.* **1997**, *124*, 67–78 and references therein.
- (18) Arata, K.; Hino, M. *Mater. Chem. Phys.* **1990**, *26*, 213–237.
- (19) Corma, A.; Martínez, A.; Martínez, C. *Appl. Catal. A* **1996**, *144*, 249–268.
- (20) Sarzanini, C.; Sacchero, G.; Pinna, F.; Signoretto, M.; Cerrato, G.; Morterra, C. *J. Mater. Chem.* **1995**, *5*, 353–360.
- (21) Bensitel, M.; Saur, O.; Lavalley, J.-C. *Mater. Chem. Phys.* **1988**, *19*, 147–156.
- (22) Escalona Platero, E.; Peñarroya Mentrut, M.; Otero Areán, C.; Zecchina, A. *J. Catal.* **1996**, *162*, 268–276.
- (23) Morterra, C.; Cerrato, G.; Bolis, V. *Catal. Today* **1993**, *17*, 505–515.
- (24) Ardizzone, S.; Bianchi, C. L.; Grassi, E. *Colloids. Surf. A* **1998**, *135*, 41–51.
- (25) The use of an acid-inert and structurally defined support-material (e.g., Aerosil SiO₂) is attractive for the preparation of heterogeneous catalysts with a high specific surface area. This facilitates their integration in reactor devices, e.g., monoliths and stirrer blades.
- (26) Some of these reactions have been mentioned in the literature.^{10,11} See also: Anderson, B. G.; Dang, Z.; Morrow, B. A. *J. Phys. Chem.* **1995**, *99*, 14444–14449; Bensitel, M.; Saur, O.; Lavalley, J. C. *Mater. Chem. Phys.* **1987**, *17*, 249–258; Jin, T.; Machida, M.; Yamaguchi, T.; Tanabe, K. *Inorg. Chem.* **1984**, *23*, 4396–4398; Yamaguchi, T.; Jin, T.; Tanabe, K. *J. Phys. Chem.* **1986**, *90*, 3148–3152.
- (27) March, J. *Advanced Organic Chemistry, Reactions, Mechanisms, and Structure*, 4th ed.; Wiley: New York, 1992; pp 765, 562 and references therein.
- (28) Tsai, T.-C.; Liu, S.-B.; Wang, I. *Appl. Catal. A* **1999**, *181*, 355–398.
- (29) Bandyopadhyay, R.; Sugi, Y.; Kubota, Y.; Rao, B. S. *Catal. Today* **1998**, *44*, 245–252.
- (30) Olah, G. A.; Kaspi, J.; Bukala, J. *J. Org. Chem.* **1977**, *42*, 4187–4191.
- (31) Dijks, I. J.; van Ochten, H. L. F.; van der Heijden, A. J. M.; Geus, J. W.; Jenneskens, L. W. *Appl. Catal. A: General* **2003**, *241*, 185–203.
- (32) Dijks, I. J.; van Ochten, H. L. F.; van Walree, C. A.; Geus, J. W.; Jenneskens, L. W. *J. Mol. Catal. A: Chem.* **2002**, *188*, 209–224.
- (33) Ikan, R. *Natural Products, A Laboratory Guide*; Israel University Press: Jerusalem, 1969; pp 137–177.
- (34) Roberts, R. M. G. *J. Chem. Soc., Perkin Trans. 2* **1976**, *10*, 1183–1190 and references therein.
- (35) Klug, H. P.; Alexander, L. E. *X-ray Diffraction Procedures For Polycrystalline and Amorphous Materials*, 2nd ed.; Wiley: New York, 1974.
- (36) Lercher, J. A. Adsorption Methods for the Assessment of the Specific Surface Area, the Pore Size Distribution and the Active Sites of

Heterogeneous Catalysts. In *Catalysis: An Integrated Approach*, 2nd ed.; Van Santen, R. A., Van Leeuwen, P. W. N. M., Moulijn, J. A., Averill, B. A., Eds.; Elsevier: Amsterdam, 1999; Chapter 13.

(37) Notice that with nonmonochromatic XPS the Zr(3d_{5/2}) and Zr(3d_{3/2}) peaks will not be resolved.

(38) Christian, G. D. *Analytical Chemistry*, 4th ed.; Wiley: New York, 1986; Chapter 6.

(39) Skoog, D. A.; West, D. M.; Holler, F. J. *Fundamentals of Analytical Chemistry*, 6th ed.; Saunders College: Philadelphia, PA, 1992; Chapter 4.

(40) Schäfer, H. *Chemical Transport Reactions*; Academic Press: New York, 1964; Translated by Frankfort, H.

(41) If the hydroxyl ions are introduced heterogeneously, nucleation and growth within the bulk of the solution can occur due to local supersaturation.^{38,39} The pH of the suspensions must be kept below 7 to prevent dissolution of the silica support.

(42) Pourbaix, M. J. N. *Atlas d'équilibres électrochimiques*; Gauthier-Villars: Paris, 1963; Zr.

(43) de Boer, M.; Leliveld, R. G.; Bruil, H. G.; van Dillen, A. J.; Geus, J. W. *Appl. Catal. A* **1993**, 102, 35–51.

(44) Alexander, L. E. *X-ray Diffraction Methods in Polymer Science*; Wiley: New York, 1969; Chapters 1 and 3.

(45) *Practical Surface Analysis, Auger and X-ray Photoelectron Spectroscopy*, 2nd ed.; Briggs, D., Seah, M. P., Eds.; Wiley: Chichester, U.K., 1990; Vol. 1.

(46) *Handbook of X-ray Photoelectron Spectroscopy*; Muilenberg, G. E., Wagner, C. D., Riggs, W. M., Davis, L. E., Moulder, J. F., Eds.; Perkin-Elmer Corporation, Physical Electronics Division: Minnesota, 1979.

(47) Price, L. S.; Parkin, I. P.; Hardy, A. M. E.; Clark, R. J. H.; Hibbert, T. G.; Molloy, K. C. *Chem. Mater.* **1999**, 11, 1792–1799.

(48) Dartigeas, K.; Benoist, L.; Gonbeau, D.; Pfister-Guillouzo, G.; Ouvrard, G.; Levasseur, A. *J. Electron Spectrosc. Relat. Phenom.* **1997**, 83, 45–58.

(49) Fairbrother, D. H.; Johnston, H.; Samorjai, G. *J. Phys. Chem.* **1996**, 100, 13696–13700.

(50) Guldán, E. D.; Schindler, L. R.; Roberts, J. T. *J. Phys. Chem.* **1995**, 99, 16059–16066.

(51) Ardizzone, S.; Bianchi, C. L.; Signoretto, M. *Appl. Surf. Sci.* **1998**, 136, 213–220.

(52) During calcination, sulfates can be eliminated. This will cause an increase of the specific surface area of the H₂SO₄/ZrO₂. At too high temperatures, however, the structure of the remaining ZrO₂ structure also collapses, which will lead to a decrease of specific area.

(53) *Gmelins Handbuch der Anorganischen Chemie*, 8. Auflage; Verlag-Chemie: Weinheim, Germany, 1960; Sulfur (SN9), Part B2, pp 668, 677.

(54) Miles, F. D.; Niblock, H.; Wilson, G. L. *Trans. Faraday. Soc.* **1940**, 36, 345–356.

(55) Kneitsch, R. *Rev. Génér. Chim. Pur. Appl.* **1902**, 5, 48–83.

(56) Nilges, J.; Schrage, J. *Fluid Phase Equilib.* **1991**, 68, 247–261.

(57) The application of the Gibbs phase rule and phase diagrams is only valid under equilibrium conditions. Hence, Figure A4 (see the Supporting Information) only provides a qualitative guideline for nonequilibrium (flow-) conditions. Because the vapor pressure of H₂O is much larger than that of H₂SO₄, in practice, there will be a negligible amount of H₂SO₄ in the vapor phase below 473 K.

(58) Bear, I. J. *Aust. J. Chem.* **1967**, 20, 415–428.

(59) Bear, I. J. *Aust. J. Chem.* **1969**, 22, 875–889.

(60) *Gmelins Handbuch der Anorganischen Chemie*, 8. Auflage; Springer-Verlag: Berlin, 1958; Zirconium (SN 42), pp 326–353.

(61) *Nouveau Traité de Chimie Minérale*; Pascal, P., Ed.; Masson: Paris, 1963; Part 9 (Zr), pp 576–621.

(62) In general, both the sulfur content and the specific area of the catalyst affect catalytic activity.^{4,9,19} See also: Katada, N.; Endo, J.; Notsu, K.; Yasunobu, N.; Naito, N.; Niwa, M. *J. Phys. Chem. B* **2000**, 104, 10321–10328. Corma, A.; Fornés, V.; Juan-Rajadell, M. I.; López Nieto, J. M. *Appl. Catal. A* **1994**, 116, 151–163.